

Mixed-valence Fluoropolytungstates

C. Sanchez and J. Livage *

Spectrochimie du Solide, Université Pierre et Marie Curie, 4 place Jussieu, 75230 Paris, France

P. Doppelt, F. Chauveau, and J. Lefebvre

Polymères Inorganiques, Université Pierre et Marie Curie, 4 place Jussieu, 75230 Paris, France

Electrochemical reduction of fluoropolytungstates leads to a new series of mixed-valence compounds. Valence trapping and electron delocalization have been studied by optical spectroscopy and e.s.r. in the temperature range 4–300 K. This shows that at low temperature the unpaired electrons are trapped on a single tungsten site. Electron delocalization occurs above 50 K. A detailed analysis of the e.s.r. linewidth dependence with temperature leads to thermal activation energies of 0.03–0.04 eV. The transfer integral J was estimated from e.s.r. and optical spectroscopy leading to $J = 0.4$ eV, which shows that the reduced fluoropolytungstates belong to the class II according to the usual classification of mixed-valence compounds.

New fluoropolytungstates have recently been prepared in our laboratory.^{1–3} They belong to the well known polyanion family, but where some oxygens have been replaced by fluorine atoms. The $[\text{HW}_{12}\text{F}_3\text{O}_{37}]^{4-}$, $[\text{H}_2\text{W}_{12}\text{F}_2\text{O}_{38}]^{4-}$, $[\text{HW}_{12}\text{F}_2\text{O}_{38}]^{5-}$, $[\text{H}_2\text{W}_{12}\text{FO}_{39}]^{5-}$, and $[\text{HW}_{12}\text{FO}_{39}]^{6-}$ fluoropolytungstates exhibit the Keggin structure⁴ (Figure 1), in which the basic unit is made up of a distorted WO_6 octahedron. Three of these octahedra share edges giving a W_3O_{13} group. Four of these groups are linked by corners around a central tetrahedral cavity containing one or two hydrogen atoms. Hydrogen-1 and ^{19}F n.m.r. experiments have shown that fluorine atoms occupy the corners of the central tetrahedral cavity.⁵

Another variety of fluoropolytungstate, $[\text{H}_2\text{W}_{18}\text{F}_6\text{O}_{56}]^{8-}$, belongs to the 2 : 18 series, the structure of which was described by Dawson.⁶ These polyanions are made up of two XW_9O_{39} sub-units that can be derived from the Keggin structure by removing one WO_6 octahedra from three different edge sharing W_3O_{13} groups (Figure 2). Two separated tetrahedral cavities are thus obtained each containing a heteroatom, X. Two basic WO_6 units can be distinguished in such a polyanion, those belonging to the W_3O_{13} caps and those belonging to the equatorial rings. Hydrogen-1 and ^{19}F n.m.r. experiments performed on $[\text{H}_2\text{W}_{18}\text{F}_6\text{O}_{56}]^{8-}$ have shown that the fluorine atoms are distributed in two groups of three among the corners of the two tetrahedral cavities surrounding the hydrogen atoms. Each of these tetrahedral cavities then has one of its faces occupied by fluoride atoms only. Two sets of tungsten sites arise from such a structure, those of WO_6 situated at the caps of the polyanions and those of WO_5F situated at the equatorial positions.

All these fluoropolytungstates can be electrochemically reduced leading to mixed-valence compounds.⁷ This paper presents a study of the electron-delocalization process in the one-electron reduced compounds, followed by e.s.r. and optical spectroscopy. Both optical and thermal activation energies are measured, allowing an estimation of the transfer integral J .

Experimental

Fluoropolytungstates⁸ have been prepared according to a procedure previously described.¹ The purity of each polyanion was checked by ^{19}F n.m.r. and elemental analysis.^{2,3,5} Electrochemical reduction was carried out under an argon atmosphere, with a mercury cathode. The imposed potential was

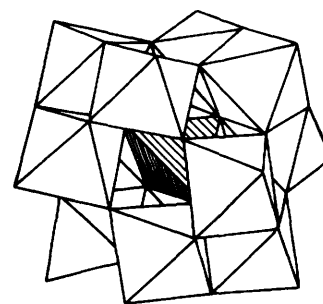


Figure 1. Structure of a $[\text{PW}_{12}\text{O}_{40}]^{3-}$ polyanion according to Keggin⁴

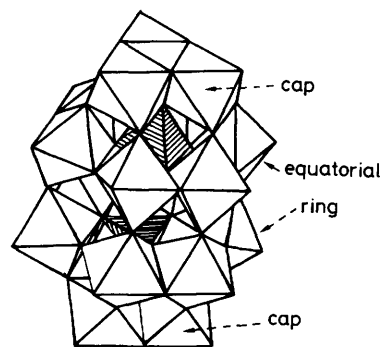


Figure 2. Structure of $[\text{P}_2\text{W}_{18}\text{O}_{62}]^{8-}$ according to Dawson⁶

given by a Tacussel PRT 500 LC. The reduction process was followed by coulometry (using an IG 5N integrator) and polarography. The reduction conditions are shown in Table 1.

Optical spectra, in the range 200–1400 nm, were recorded at room temperature on a Beckman spectrometer. X-Band e.s.r. spectra were recorded on a JEOL ME 3X spectrometer in the temperature range 4–300 K. Magnetic field measurements were made by using an n.m.r. proton probe.

Results

(a) *Electron Spin Resonance.*—The e.s.r. spectrum of a frozen solution of the one-electron reduced $[\text{H}_2\text{W}_{18}\text{F}_6\text{O}_{56}]^{9-}$ polyanion is shown in Figure 3(a). At 4 K, this spectrum is typical of a W^{V} ion in a rhombic ligand field. No hyperfine

Table 1. Reduction conditions of the fluoropolytungstate polyanions

Polyanion	Media ^a	Reduction potential ^b (mV)
[H ₂ W ₁₈ F ₆ O ₅₆] ⁸⁻	HCl (0.1); NaCl (1)	-150
[HW ₁₂ FO ₃₉] ⁶⁻	Succinic buffer (0.5) pH = 6; NaCl (1)	-680
[HW ₁₂ F ₂ O ₃₈] ⁵⁻	Acetic buffer (0.5) pH = 5; NaCl (1)	-530
[H ₂ W ₁₂ FO ₃₉] ⁵⁻		
[HW ₁₂ F ₃ O ₃₇] ⁴⁻	HCl (0.1); NaCl (1)	-330
[H ₂ W ₁₂ F ₂ O ₃₈] ⁴⁻		

^a Concentrations in mol dm⁻³ in parentheses. ^b versus Calomel electrode.

Hamiltonian, equation (1), where x , y , and z refer to the main

$$\mathcal{H} = g_x \beta H_x S_x + g_y \beta H_y S_y + g_z \beta H_z S_z \quad (1)$$

axis of the rhombic g tensor. The magnetic parameters are obtained by computer simulation with a Gaussian lineshape [Figure 3(b)], and are reported in Table 2.

The temperature dependence of the e.s.r. spectrum is shown in Figure 4(a). A line broadening is observed above 45 K. The spectrum first appears axial before being wholly isotropic. The two high-field components collapse first suggesting that g_x and g_y are smaller than g_z . The temperature variation of the e.s.r. spectrum was better simulated by keeping the three g values constant and varying only the linewidth and lineshape [Figure 4(b)]. The best fit was obtained for a Gaussian lineshape below 45 K and a Lorentzian one above 120 K. In between, both shapes had to be taken into account.

Table 2. Electron spin resonance parameters of reduced polytungstates and fluoropolytungstates

Polyanion	Temp. (K)	g_x	g_y	g_z	$\alpha^2\beta^2$	$\alpha^2\gamma^2$	$E_{\text{opt.}}/\text{eV}$	Ref.
[HW ₁₂ F ₃ O ₃₇] ⁵⁻	4	1.853	1.821	1.778	0.81	0.73	1.05	This work
[H ₂ W ₁₂ F ₂ O ₃₈] ⁵⁻	4	1.857	1.822	1.781	0.77	0.69	1.07	This work
[HW ₁₂ F ₂ O ₃₈] ⁶⁻	4	1.854	1.819	1.768	0.82	0.70	1.05	This work
[H ₂ W ₁₂ FO ₃₉] ⁶⁻	4	1.850	1.812	1.767	0.82	0.76	1.05	This work
[HW ₁₂ FO ₃₉] ⁷⁻	4	1.852	1.807	1.753	0.82	0.80	1.05	This work
[H ₂ W ₁₂ O ₄₀] ⁷⁻	4	1.852	1.805	1.759				7
[H ₂ W ₁₈ F ₆ O ₅₆] ⁹⁻	4	1.811	1.852	1.917	0.72	0.75	1.37	This work
[P ₂ W ₁₈ O ₆₂] ⁷⁻	26	1.814	1.854	1.906				7
[As ₂ W ₁₈ O ₆₂] ⁷⁻	12	1.811	1.852	1.917				7

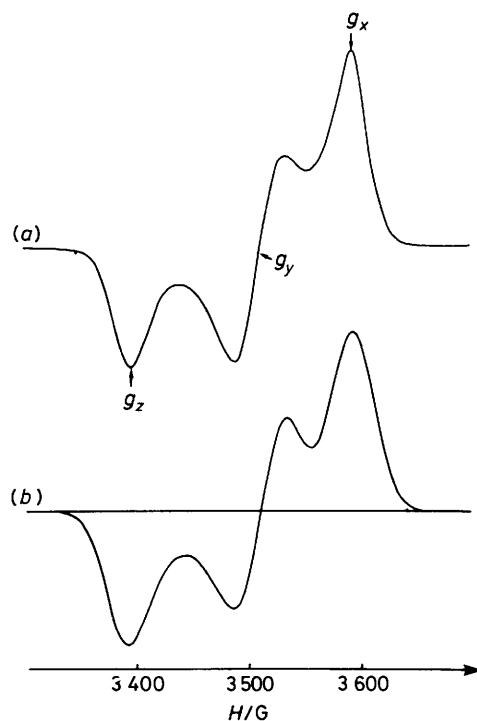


Figure 3. E.s.r. spectrum of the one-electron reduced [H₂W₁₈F₆O₅₆]⁹⁻ polyanion recorded at 4 K: (a) experimental and (b) simulated

coupling with the 14% abundant ¹⁸³W isotope ($I = \frac{1}{2}$) or fluorine ¹⁹F ($I = \frac{1}{2}$) ligands is observed. This is probably due to the linewidth which is quite large ($\Delta H = 36$ G). The e.s.r. spectrum can then be described with a Zeeman spin

The e.s.r. spectrum of a frozen solution of the one-electron reduced [HW₁₂F₃O₃₇]⁵⁻ polyanion is shown in Figure 5(a). At 4 K, it corresponds to a W^V ion in a rhombic ligand field. No hyperfine structure is observed and the spectrum can be described with the same spin Hamiltonian as previously

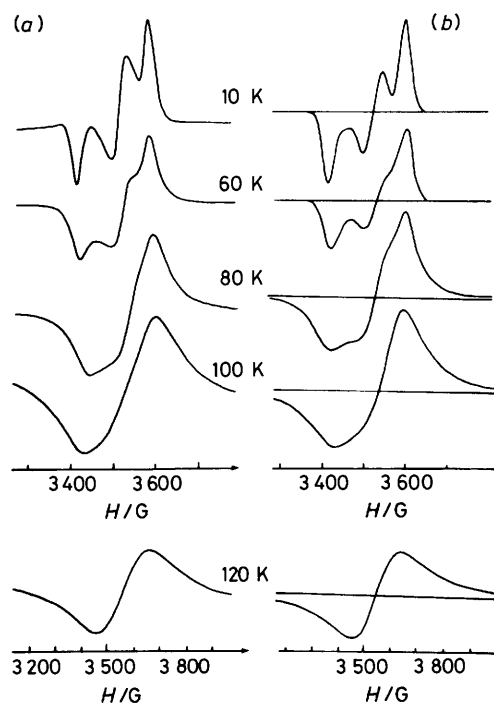


Figure 4. Temperature dependence of the e.s.r. spectra of [H₂W₁₈F₆O₅₆]⁹⁻: (a) experimental and (b) simulated

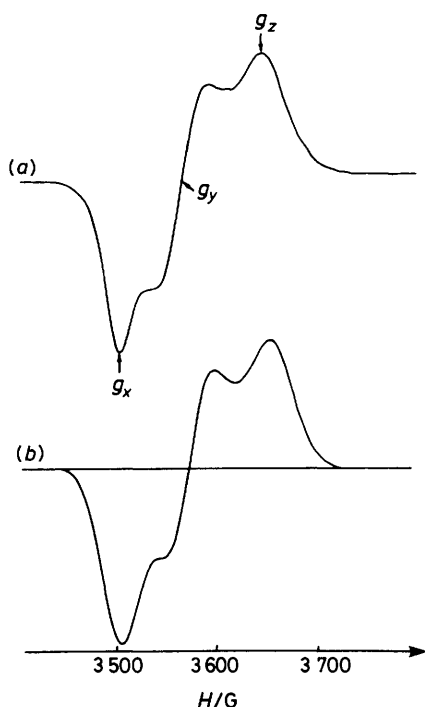


Figure 5. E.s.r. spectrum of the one-electron reduced $[\text{HW}_{12}\text{F}_3\text{O}_{37}]^{5-}$ polyanion recorded at 4 K: (a) experimental and (b) simulated

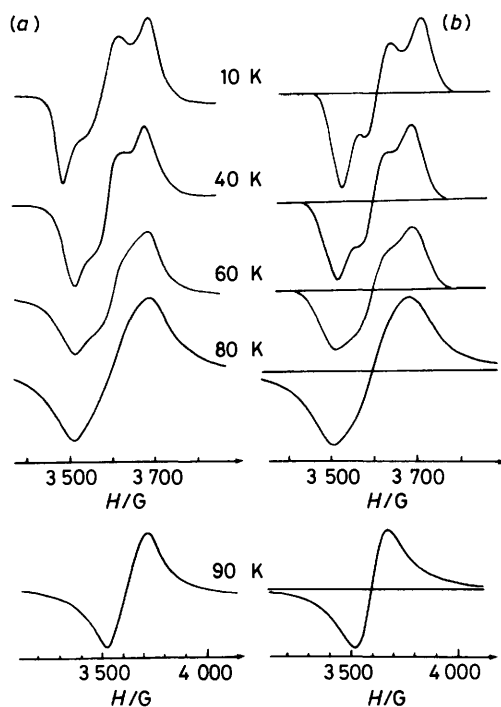


Figure 6. Temperature dependence of the e.s.r. spectra of $[\text{HW}_{12}\text{F}_3\text{O}_{37}]^{5-}$: (a) experimental and (b) simulated

[equation (1)]. The magnetic parameters were determined by computer simulation using a Gaussian lineshape [Figure 5(b)] and are also reported in Table 2. A line broadening is observed above 35 K [Figure 6(a)]. As previously, the e.s.r. spectrum first appears axial before being wholly isotropic above 90 K, but in this case, the two low-field components col-

Table 3. Spectral data for reduced fluoropolytungstates in the u.v.-visible and near-i.r. region

Polyanion	$\nu_{\text{max.}}/\text{cm}^{-1}$ ($\epsilon/\text{dm}^3 \text{ mol}^{-1} \text{ cm}^{-1}$)
$[\text{HW}_{12}\text{F}_3\text{O}_{37}]^{5-}$	8 400 (1 930), 14 200 (2 590), 19 600 (1 630), 38 200 (37 920)
$[\text{H}_2\text{W}_{12}\text{F}_2\text{O}_{38}]^{5-}$	8 600 (1 825), 13 900 (2 420), 19 100 (1 490), 38 300 (41 375)
$[\text{HW}_{12}\text{F}_2\text{O}_{38}]^{6-}$	8 500 (1 080), 14 100 (1 920), 19 800 (1 100), 38 500 (38 880)
$[\text{H}_2\text{W}_{12}\text{FO}_{39}]^{6-}$	8 300 (1 340), 14 300 (2 040), 19 100 (1 055), 38 500 (39 190)
$[\text{HW}_{12}\text{FO}_{39}]^{7-}$	8 500 (1 130), 14 800 (1 785), 19 100 (860), 38 200 (38 400)
$[\text{H}_2\text{W}_{18}\text{F}_6\text{O}_{56}]^{9-}$	11 000 (2 938), 14 300 (2 700), 17 200 (1 670), 39 000 (44 280)

lapse first suggesting that g_x and g_y are now larger than g_z . Such an inversion has already been observed with corresponding non-fluorinated oxopolytungstates.⁸ The computer simulation was still performed by keeping the g components constant, with a Gaussian lineshape below 50 K and a Lorentzian one above 90 K.

The e.s.r. spectra obtained with the other Keggin fluoropolytungstates $[\text{H}_2\text{W}_{12}\text{F}_2\text{O}_{38}]^{5-}$, $[\text{HW}_{12}\text{F}_2\text{O}_{38}]^{6-}$, $[\text{H}_2\text{W}_{12}\text{FO}_{39}]^{6-}$, and $[\text{HW}_{12}\text{FO}_{39}]^{7-}$ are quite similar. The corresponding g values are also reported in Table 2.

(b) *Optical Spectra.*—The optical absorption bands of the one-electron reduced fluoropolytungstates are reported in Table 3. The corresponding fully oxidized polyanions give an intense absorption in the u.v. region only, around 38 000–39 000 cm^{-1} .^{1–3} These bands correspond to allowed charge-transfer transitions from molecular orbitals mainly localized on tungsten ions. They can still be seen in the optical spectra of the reduced species.

Intervalence bands corresponding to an electron transition between W^{V} and W^{VI} ions are observed in the red part of the spectrum, between 8 000 and 11 000 cm^{-1} . Shoulders can be seen around 13 500 and 20 000 cm^{-1} . Their attribution is not obvious but we may think that they correspond to $d-d$ transitions.

Discussion

(a) *Electron Localisation at Low Temperature.*—Electron spin resonance spectra show that at low temperature the unpaired electron remains localized on a single tungsten site (Figures 3 and 5), but the question arises whether this tungsten has a fluorine neighbour or not? If yes, a superhyperfine coupling should be expected, as in WOF_5 where it leads to a splitting of ca. 14 G.⁹ The $J(\text{W-F})$ couplings of 10 or 46 Hz have been measured previously in our compounds by n.m.r.,⁷ but our e.s.r. experiments do not reveal any hyperfine coupling, even at very low temperatures. It must then be smaller than the linewidth, i.e. $a_{\text{F}} < 30$ G. This is not unexpected as the unpaired electron lies in a d_{xy} orbital (see below). No overlapping can then occur with the p orbitals of the fluorine atom situated on the z axis of the WO_2F octahedron. The hyperfine coupling is then mainly dipolar and a rough calculation, taking a W-F distance¹⁰ of 2.3 Å, shows that $a_{\text{F}} = g_e \beta_e g_n \beta_n r^{-3} \sim 4$ G, a much lower value than the observed linewidth. ENDOR experiments are performed in order to verify this assumption.

Nevertheless, in the case of $[\text{H}_2\text{W}_{18}\text{F}_6\text{O}_{56}]^{9-}$, the unpaired electron may occupy two different tungsten sites; those

situated at the caps of the polyanion or those situated around the polyanion belt. Previous reports suggest that it should be trapped on one of the equatorial tungstens.^{8,11} Our experiments agree with such a result. The g values found for the 2:18 fluoropolytungstates are very close to those found for the non-fluorinated ones. They show that the local symmetry around the W^V ion is quite different in both the Keggin and Dawson polyanions (Table 2). As the W_3O_{13} groups are quite similar in both polyanions, we think that the unpaired electron may be trapped on one of the equatorial tungstens.

(b) *Ground State Delocalization.*—The e.s.r. spectra of the one-electron reduced fluoropolytungstates show that at low temperature the unpaired electron is trapped on a single tungsten site. It is then possible, from low-temperature data together with optical transitions, to obtain information regarding the degree of valence trapping in the ground and excited states.

The rhombic symmetry of the g tensor shows that the site symmetry is strongly distorted so that all degeneracies are removed. The ligand-field symmetry around W^V can be approximated to C_{2v} . The short $W=O$ double bond yields a destabilization of all z components so that the d_{xy} orbital lies lower. The ground state can then be described by equation (2) and the first excited states by equations (3) and (4), where ψ_i

$$|A_2\rangle = \alpha|d_{xy}\rangle + \alpha'|\psi_{A_2}\rangle \quad (2)$$

$$|B_1\rangle = \beta|d_{xz}\rangle + \beta'|\psi_{B_1}\rangle \quad (3)$$

$$|B_2\rangle = \gamma|d_{yz}\rangle + \gamma'|\psi_{B_2}\rangle \quad (4)$$

represent the combination of ligand orbitals having the right symmetry.

The two $d-d$ transitions observed in the visible region presumably correspond to the ${}^2B_1 \leftarrow {}^2A_2$ and ${}^2B_2 \leftarrow {}^2A_2$ transitions. Transitions toward the higher excited state $|A_1\rangle$ should lie in the near-u.v. region where they are hidden by charge-transfer transitions. Such an attribution still remains debatable, but it seems to agree quite well with our e.s.r. results and leads to reasonable values of the α , β , and γ parameters.

The g value for an unpaired d_{xy} electron in a C_{2v} ligand

$$g_x = g_e - \frac{2\alpha^2\beta^2\lambda^0}{E_{B_1} - E_{A_2}} \quad (5)$$

$$g_y = g_e - \frac{2\alpha^2\gamma^2\lambda^0}{E_{B_2} - E_{A_2}} \quad (6)$$

field can be expressed by equations (5) and (6) where λ^0 corresponds to the free ion spin-orbit coupling and depends on the effective charge carried by the tungsten atom. A value of $\lambda^0 = 1800 \text{ cm}^{-1}$ corresponding to a W^{3+} ion is usually taken in such compounds leading to the $\alpha^2\beta^2$ and $\alpha^2\gamma^2$ values reported in Table 2.

These values appear to be somewhat larger in 2:18 fluorotungstates than in the 12-tungstates, indicating a smaller degree of delocalization in the ground state.⁹ This agrees with the fact that the e.s.r. lines broaden in a different way and with the blue shift of the intervalence charge-transfer bands. Such a valence trapping could be explained by the greater degree of distortion of the W^V sites in the 2:18 fluorotungstates.

(c) *Electron Delocalization.*—The reduced fluoropolytungstates are mixed-valence compounds. A hopping of the unpaired electrons may be expected between the W^V and W^{VI} ions. Such a hopping process can be either optically activated, leading to the intervalence charge-transfer bands around

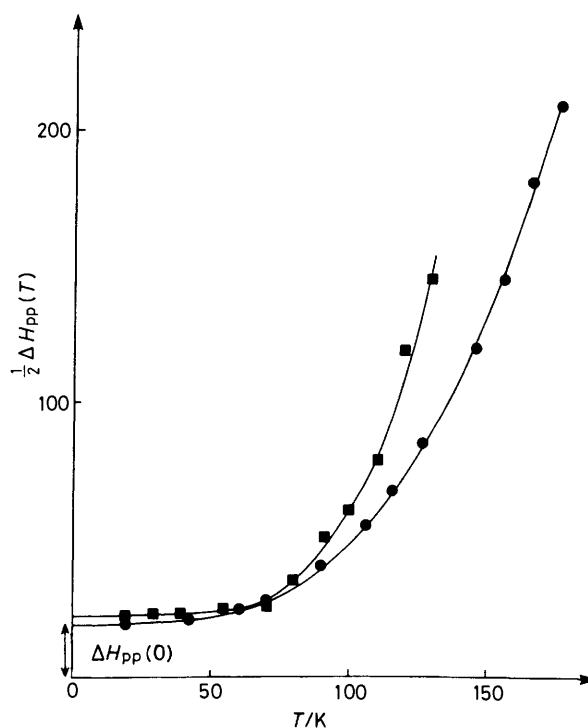


Figure 7. Temperature dependence of the e.s.r. linewidth (G) of $[H_2-W_{18}F_6O_{56}]^{9-}$ (●) and $[HW_{12}F_3O_{37}]^{5-}$ (■). $\frac{1}{2}\Delta H_{pp}(T)$ corresponds to the peak-to-peak half-width (G)

$10\,000 \text{ cm}^{-1}$, or thermally activated leading to a broadening of the e.s.r. signal above 50 K.

The optical activation energies E_{opt} are usually deduced from the position of the intervalence charge transfer band. They are reported in Table 2. The thermal activation energies are much more difficult to measure. They can however be deduced from a careful analysis of the e.s.r. linewidth dependence with temperature. The peak-to-peak linewidth $\Delta H_{pp}(T)$ can be expressed as the sum of two terms,^{12,13} equation (7),

$$\Delta H_{pp}(T) = \Delta H_{pp}(0) + \delta H_{pp}(T) \quad (7)$$

where the temperature independent linewidth $\Delta H_{pp}(0)$ arises from dipolar interactions between paramagnetic ions together with non-resolved hyperfine interactions and ligand-field distributions. It corresponds to the linewidth at 0 K and can be obtained by extrapolation of the $\Delta H_{pp}(T) = f(T)$ plot [Figure 7].

The temperature dependent linewidth $\delta H_{pp}(T)$ is due to a lifetime broadening arising from spin-lattice relaxations induced by the electron hopping.¹⁴ The e.s.r. linewidth $1/t_2'$ [equation (8)] depends on the relaxation times. At low

$$\frac{1}{t_2'} = \frac{1}{t_2} + \frac{1}{2t_1} \quad (8)$$

temperature, t_1 is rather long and the linewidth is dominated by spin-spin interactions; t_1 decreases with temperature and when $1/2t_1$ becomes larger than $1/t_2$ a line broadening is observed that depends on the lifetime of the spin state. We can then write $\delta H_{pp}(T) = C\nu_h$ where ν_h is the hopping frequency of the unpaired electron and C a proportionality factor. Mott¹³ has derived an expression for the hopping frequency of electrons in mixed-valence compounds [equation (9)].

$$\nu_h = \nu_0 \exp(-2\alpha R) \exp(-E_{th}/kT) \quad (9)$$

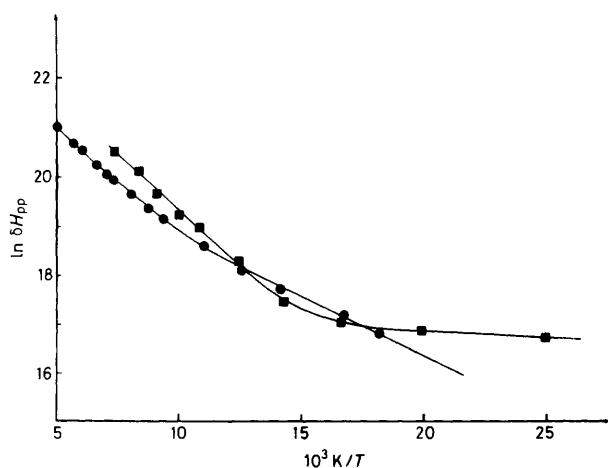


Figure 8. Plot of $\ln \delta H_{pp} = f(T^{-1})$ where δH_{pp} corresponds to the temperature dependent part of the e.s.r. linewidth: $[\text{H}_2\text{W}_{18}\text{F}_6\text{O}_{56}]^{9-}$ (●) and $[\text{HW}_{12}\text{F}_3\text{O}_{37}]^{5-}$ (■)

The first exponential, where α is the rate of the wavefunction decay and R the W-W distance, corresponds to a tunnel effect. The second exponential corresponds to the thermally activated hopping.

A linear plot of $\ln \delta H_{pp}$ versus T^{-1} is observed in the high-temperature region, where $1/2t_1$ is much larger than $1/t_2$ [Figure 8]. Its slope gives a thermal activation energy E_{th} . Such an analysis was performed for two fluoropolytungstates to give $E_{th} = 0.040$ eV for $[\text{H}_2\text{W}_{18}\text{F}_6\text{O}_{56}]^{9-}$ and $E_{th} = 0.038$ eV for $[\text{HW}_{12}\text{F}_3\text{O}_{37}]^{5-}$.

A relationship between the optical ($E_{opt.}$) and thermal activation ($E_{th.}$) energies can be established in the class II mixed-valence compounds.¹⁵ In the limit of a vanishing electronic interaction between metal sites, the thermal energy should be *ca.* $\frac{1}{4}$ of the optical energy. This is no longer true when the transfer integral J between both sites becomes important; we then have¹⁶ equation (10).

$$J = \frac{1}{2}E_{opt.} - (E_{opt.}E_{th.})^{\frac{1}{2}} \quad (10)$$

In our case this expression would lead to transfer integrals of $J = 0.45$ eV for $[\text{H}_2\text{W}_{18}\text{F}_6\text{O}_{56}]^{9-}$ and $J = 0.31$ eV for $[\text{HW}_{12}\text{F}_3\text{O}_{37}]^{5-}$. These values are quite high when compared with molybdate and vanadate polyanions.^{17,18} This is probably due to the larger extent of the 5d tungsten orbitals.

References

- 1 F. Chauveau, P. Doppelt, and J. Lefebvre, *Inorg. Chem.*, 1980, **19**, 2803.
- 2 F. Chauveau, P. Doppelt, and J. Lefebvre, *J. Chem. Res.*, 1981, (S) 155, (M) 1937.
- 3 P. Doppelt and J. Lefebvre, *Nouv. J. Chim.*, 1981, **5**, 463.
- 4 J. F. Keggin, *Nature (London)*, 1933, **131**, 909.
- 5 F. Chauveau, P. Doppelt, and J. Lefebvre, *J. Chem. Res.*, 1978, (S) 130, (M) 1727.
- 6 B. Dawson, *Acta Crystallogr.*, 1953, **6**, 115.
- 7 J. Lefebvre, F. Chauveau, P. Doppelt, and C. Brevard, *J. Am. Chem. Soc.*, 1981, **103**, 4589.
- 8 R. A. Prados and M. P. Pope, *Inorg. Chem.*, 1976, **15**, 2547.
- 9 J. T. C. Van Kemenade, *Rec. Trav. Chim. Pays-Bas*, 1973, **92**, 1102.
- 10 H. D'Amour, *Acta Crystallogr., Sect. B*, 1976, **32**, 769; J. Fuchs and E. P. Flindt, *Z. Naturforsch., Teil B*, 1979, **34**, 412.
- 11 R. Acerete, S. Harmalker, C. F. Hammer, M. T. Pope, and L. C. W. Baker, *J. Chem. Soc., Chem. Commun.*, 1979, 777.
- 12 B. Movaghar and L. Schweitzer, *Phys. Status Solidi B*, 1977, **80**, 491.
- 13 N. F. Mott, *Adv. Phys.*, 1967, **16**, 49.
- 14 R. Bachus, B. Movaghar, L. Schweitzer, and U. Voget-Grote, *Philos. Mag. B*, 1979, **39**, 27.
- 15 N. S. Hush, *Prog. Inorg. Chem.*, 1967, **8**, 391.
- 16 N. S. Hush, *Mixed Valence Compounds*, ed. D. B. Brown, NATO Advanced Study Institute series, D. Reidel, 1979, p. 151.
- 17 C. Sanchez, J. Livage, J. P. Launay, M. Fournier, and Y. Jeannin, *J. Am. Chem. Soc.*, 1982, **104**, 3194.
- 18 N. Gharbi, C. Sanchez, J. Livage, J. Lemerle, L. Nejem, and J. Lefebvre, *Inorg. Chem.*, 1982, **21**, 2758.

Received 24th March 1982; Paper 2/514